

## Fluctuating Velocity and Momentum Transfer in Dense Granular Flows

G. Gioia and S. E. Ott-Monsivais

*Department of Theoretical and Applied Mechanics, University of Illinois, Urbana, Illinois 61801, USA*

K. M. Hill

*St. Anthony Falls Laboratory, University of Minnesota, Minneapolis, Minnesota 55455, USA*

(Received 15 May 2005; published 6 April 2006)

We show experimentally that in a free-surface granular flow the fluctuating velocity brings about momentum transfer at a considerable rate only very close to the free surface. Away from the free surface, where the flow is dense and stratified (or laminar), the fluctuating velocity plays no prominent dynamic role and stems passively from a kinematic constraint: The strata of particles must shake laterally as they slip past one another in the direction of the mean flow. Based on this insight, we formulate a simple model for the fluctuating velocity of dense granular flows. The predictions of the model agree well with our experimental measurements.

DOI: [10.1103/PhysRevLett.96.138001](https://doi.org/10.1103/PhysRevLett.96.138001)

PACS numbers: 45.70.-n

In fluid dynamics, the velocity fields are customarily split into two additive components, the mean velocity and the fluctuating velocity [1]. The fluctuating velocity has been studied extensively in liquid flows—where it has a strong effect on the transfer of mass, heat, and momentum [2]—but not so extensively in granular flows. Yet, in spite of the differences between granular and liquid flows, the effect of the fluctuating velocity may be just as strong in granular flows as in liquid flows and relevant to many technological processes and natural phenomena that involve granular matter [3].

One notable difference between granular flows and liquid flows concerns precisely the fluctuating velocity. In granular flows, there is usually a fluctuating velocity [4]. In liquid flows, however, there is a fluctuating velocity only if the mean velocity is high enough for the flow to be turbulent [5]. In the case of liquid flows, the advent of a fluctuating velocity signals a switch in the shear stress-producing mechanism [2]. Where the mean velocity is low, the shear stress  $\tau$  stems from the viscosity. Then  $\tau = \mu\dot{\gamma}$ —the Newton stress, where  $\mu$  is the viscosity and  $\dot{\gamma}$  the shear strain rate. Where the mean velocity is high, the production of shear stress becomes rapidly dominated by the momentum transfer effected by the fluctuating velocity. Then  $\tau = \rho\overline{u'v'}$ —the Reynolds stress, where  $\rho$  is the density,  $u'$  and  $v'$  are mutually orthogonal components of the fluctuating velocity, and  $\overline{(\cdot)}$  denotes time average [2]. Because of this marked dependence on the mean velocity, the stress-producing mechanisms are spatially disjoint in a liquid flow. For example, in a pipe flow, the Newton stress is dominant close to the wall and the Reynolds stress away from the wall.

Since a granular flow is usually “turbulent” (in the sense that it usually contains a fluctuating velocity), it might be thought that the Reynolds stress [6] contributes a sizable fraction of the applied stress everywhere in the flow. Yet in this Letter we show that, just as is the case in liquid flows,

in free-surface granular flows the stress-producing mechanisms are spatially disjoint: The momentum transfer is appreciable close to the free surface, but away from the free surface, where the mean velocity is low and the flow dense, the Reynolds stress accounts for only a small fraction of the applied stress. This result suggests that, in dense granular flows, the fluctuating velocity is mostly passive and, further, that the fluctuating velocity, the shear strain rate, and the structure of the flow are connected by a purely kinematic relation.

In our experiments, we use a transparent drum of diameter 30 cm halfway filled with spherical plastic or steel beads of diameter  $d = 2$  or 3 mm. The depth of the drum is about  $2.5d$ . We rotate the drum about its axis with angular velocities  $\omega = 1$  to 1.5 rpm. At these angular velocities, the beads move relative to one another only in a steady, shallow surficial layer—the flowing layer [7]—whose free surface forms a constant angle  $\alpha$  with the horizon [Fig. 1(a)]. We focus a digital camera on the deepest portion of the flowing layer, where the flow is uniform in the  $x$  direction, and collect 1024 images at a rate of 500 Hz. Subsequently, we use a computer program [8] to determine the coordinates of each individual bead center in each image (with a resolution better than  $d/100$ ) and evaluate the velocity vectors of the bead centers throughout the experiment [Fig. 1(b)] as well as the trajectories of the bead centers [Figs. 1(c) and 1(d)]. Last, we use a simple method [9] to compute six Eulerian fields: the mean volume fraction of beads  $\bar{f}(y)$ , the mean velocity  $\bar{u}(y)$ , the Reynolds normal stress  $\overline{\sigma_{Re}(y)} = \overline{f'v'(y)}$ , the Reynolds shear stress  $\tau_{Re}(y) = \overline{fu'v'(y)}$ , the applied normal stress  $\sigma_a(y) = g \cos\alpha \int_0^y \bar{f}(\eta) d\eta$ , and the applied shear stress  $\tau_a(y) = g \sin\alpha \int_0^y \bar{f}(\eta) d\eta$ . Here  $y$  is the depth within the flowing layer,  $u$  and  $v$  are the velocities in the  $x$  and  $y$  direction, respectively,  $u' = u - \bar{u}$  and  $v' = v - \bar{v} = v$  are the fluctuating velocities,  $g$  is the gravitational acceleration, and the stresses are normalized by the density of

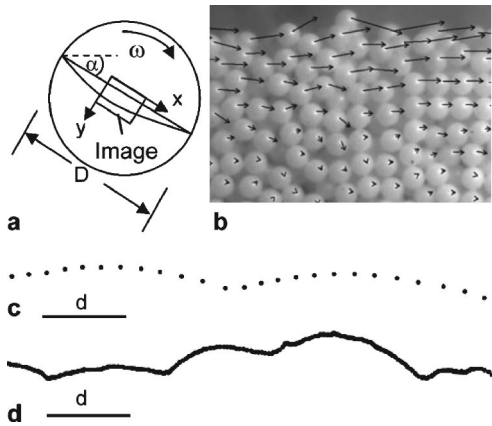


FIG. 1. (a) Schematic of the partially filled rotating drum. Inside the flowing layer (indicated in the figure), the beads move primarily parallel to the free surface, from left to right in the  $x$  direction. Outside the flowing layer, the beads move in solidlike rotation with the drum. The rectangle marks the area covered by the video images. (b) Instantaneous velocity vectors drawn on part of an image from an experiment with plastic beads,  $d = 2$  mm, and  $\omega = 1$  rpm. (In reality, these are average velocity vectors between two successive images.) Trajectory of a bead center at a depth (c)  $y \approx 1d$  (in the upper part of the flowing layer) and (d)  $y \approx 5d$  (in the lower part of the flowing layer).

the beads. In Fig. 2, we plot the Eulerian fields from a representative experiment.

Figure 2(a) suggests that the flowing layer may be divided into two parts. The upper part is marked by a variable  $\bar{f}(y)$ ; it extends from the top of the flowing layer to a depth  $y \approx 2d$ . The lower part is marked by a constant  $\bar{f}(y)$ ; it extends from  $y \approx 2d$  to the bottom of the flowing layer ( $y \approx 8d$ ). The image in Fig. 1(b) suggests that, in the upper part of the flowing layer, the flow is sparse (as opposed to dense). A bead in the sparse flow makes brief sporadic contacts with neighboring beads as it moves forward with high  $\bar{u}$  [Fig. 1(c)]. These contacts are collisional and can effect considerable momentum transfer. Thus, the Reynolds stresses account for a sizable fraction of the applied stresses in the upper part of the flowing layer [Figs. 2(c) and 2(d)]. On the other hand, the image in Fig. 1(b) suggests that, in the lower part of the flowing layer, the flow is dense. A bead in the dense flow makes simultaneous prolonged contacts with several neighboring beads as it moves forward with low  $\bar{u}$  [Fig. 1(d)]. These contacts are noncollisional and cannot effect considerable momentum transfer. Thus, the Reynolds stresses account for a negligible fraction of the applied stresses in the lower part of the flowing layer [Figs. 2(c) and 2(d)].

From the previous paragraph, we conclude that over most of the flowing layer the granular flow is dense, the mean volume fraction is constant, and the Reynolds stresses are negligible. We identify this dense granular flow of constant  $\bar{f}$  with the “solidlike regime” of Orpe and Khakhar [10]. These authors have remarked that the solid-

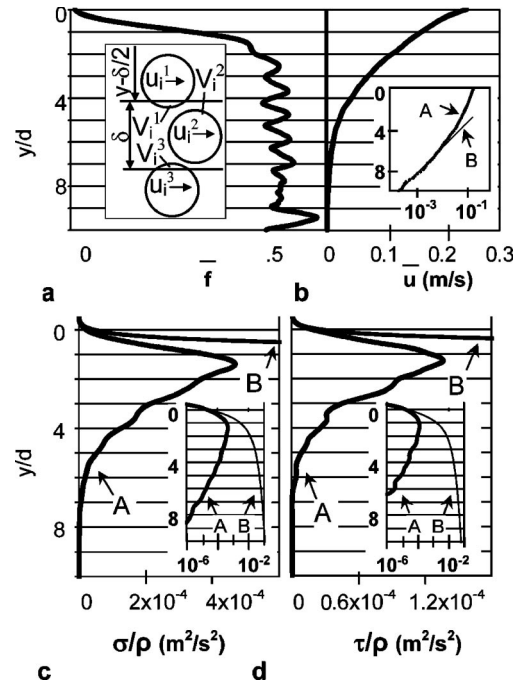


FIG. 2. Eulerian fields from an experiment with plastic beads,  $d = 3$  mm, and  $\omega = 1$  rpm. (a) Mean volume fraction. (For comparison, in a square packing  $\bar{f} = 0.524$ , and in a hexagonal packing  $\bar{f} = 0.605$ .) The inset illustrates the method of computation of the fields [9]. (b) Mean velocity. Inset: The same in a linear-log plot (A), showing that for  $y > 6d$  the decay is exponential with a decay length of  $1.1d$  (B), in good agreement with the experiments of Ref. [17]. (c) Reynolds (A) and applied (B) normal stress (normalized by the density of the beads). Inset: The same, plotted using a linear-log scale. (d) Reynolds (A) and applied (B) shear stress (normalized by the density of the beads). Inset: The same, plotted using a linear-log scale.

like regime can be modeled using the theory of plasticity. The same conclusion holds for the dense granular flow, in which the dominant shear stress-producing mechanism—friction—is suitably described by the theory of plasticity of Mohr and Coulomb, for example [11].

We have established that the fluctuating velocity does not play a prominent dynamic role in dense granular flow. We surmise that the fluctuating velocity is the passive outcome of a kinematic constraint: In a dense granular flow, a bead is always in contact with its neighboring beads, and to slip past them it must find its way around them, tracing a circuitous trajectory as it deviates now and again from the direction of the mean velocity. A mathematical description of this scenario is facilitated by the structure of the dense granular flow, in which the beads are arranged in strata parallel to the free surface of the flowing layer. [A telling signature of the stratified structure of the flow is apparent in the plot of  $\bar{f}(y)$  in Fig. 2(a), in the form of an oscillation of wavelength equal to one bead diameter—the distance between adjacent strata of beads [12].] Let us number the strata of beads starting with 0 for the

stratum at the bottom of the flowing layer. (Thus, the mean velocity of stratum 0 is zero,  $\bar{u}_0 = 0$ , and the mean velocity of stratum 1 is positive,  $\bar{u}_1 > 0$ .) As stratum  $i$  slips on the wavy surface of stratum  $i - 1$  (Fig. 3), the beads in stratum  $i$  must shake relative to the beads in stratum  $i - 1$  with a frequency  $\nu_i = \Delta\bar{u}_i/d$  and a maximum shaking velocity proportional to  $\Delta\bar{u}_i$ , where  $\Delta\bar{u}_i = \bar{u}_i - \bar{u}_{i-1}$ . For simplicity, we assume the shaking velocity to be harmonic in time. Then we can write an expression for the shaking velocity in the  $y$  direction in the form  $\Delta v'_i = \xi_v \Delta\bar{u}_i \cos(2\pi\nu_i t)$ , where  $\xi_v$  is a proportionality constant. Because each stratum slips over the one below it, the beads in stratum  $i$  shake in the  $y$  direction relative to the beads at the bottom of the flowing layer with a total shaking velocity  $\sum_{k=1}^{k=i} \Delta v'_k$ , which we identify with  $v'_i$ , the  $y$  component of the fluctuating velocity at the depth of stratum  $i$ . Thus,  $v'_i = \xi_v \sum_{k=1}^{k=i} \Delta\bar{u}_k \cos(2\pi\nu_k t)$ . In a similar manner, we can compute the  $x$  component of the fluctuating velocity at the depth of stratum  $i$  as  $u'_i = \xi_u \sum_{k=1}^{k=i} \Delta\bar{u}_k \cos(2\pi\nu_k t + \phi)$ , where  $\xi_u$  is a proportionality constant and  $\phi$  is a phase angle between the shakings in the  $y$  and the  $x$  directions.

To compare the predictions of the slip-and-shake model of the previous paragraph with our experimental measurements, we evaluate the correlations  $\overline{v'_i v'_i}$ ,  $\overline{u'_i u'_i}$ , and  $\overline{u'_i v'_i}$ . For example,  $\overline{v'_i v'_i} \equiv \lim_{T \rightarrow \infty} (1/T) \int_0^T v'_i v'_i dt = (1/2) \xi_v^2 \sum_{k=1}^{k=i} \sum_{l=1}^{l=i} \Delta\bar{u}_k \Delta\bar{u}_l \delta_{kl} = (1/2) \xi_v^2 \sum_{k=1}^{k=i} (\Delta\bar{u}_k)^2$ , where we have taken into account that  $2 \lim_{T \rightarrow \infty} (1/T) \times \int_0^T \cos(2\pi\nu_k t) \cos(2\pi\nu_l t) dt = \delta_{kl}$ —the Kröner delta function [ $\delta_{kl} = 1$  for  $k = l$  and  $\delta_{kl} = 0$  for  $k \neq l$ ]. To derive a theoretical expression for the field  $\overline{v' v'}(y)$  in terms of the shear strain rate,  $\dot{\gamma}(y) = d\bar{u}(y)/dy$ , we write  $\Delta\bar{u}_k = \dot{\gamma}_k d$  and turn the sum over the strata into an integral across the flowing layer [13], with the final result

$$\overline{v' v'}(y) = \xi_v^2 \frac{d}{2} \int_y^{y_b} \dot{\gamma}^2(\eta) d\eta, \quad (1)$$

where  $y_b$  is the depth at the bottom of the flowing layer. By proceeding in a similar way, we conclude that

$$\overline{u' u'}(y) = \xi_u^2 \frac{d}{2} \int_y^{y_b} \dot{\gamma}^2(\eta) d\eta \quad (2)$$

and

$$\overline{u' v'}(y) = \xi_u \xi_v \cos\phi \frac{d}{2} \int_y^{y_b} \dot{\gamma}^2(\eta) d\eta. \quad (3)$$

To obtain values for  $\xi_v$ ,  $\xi_u$ , and  $\phi$ , we fit the correlations of (1)–(3), respectively, to the corresponding experimental

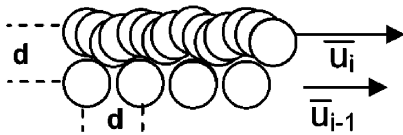


FIG. 3. Simplified geometry of the “slip-and-shake” model.

correlations [14]. Since (1)–(3) apply only where the flow is dense, we perform the fits over the lower part of the flowing layer, starting at a nominal depth of  $2d$ . [To compute the integrals of (1)–(3), we use the experimental  $\dot{\gamma}(y)$ .] For example, for an experiment with plastic beads,  $d = 2$  mm, and  $\omega = 1$  rpm, we obtain  $\xi_v = 0.9$ ,  $\xi_u = 1.2$ , and  $\phi = 1.4$  rad. Figure 4(a) shows that the attendant fit is quite good (for  $y > 2d$ ). In particular, the model predicts very low-amplitude oscillations in  $\overline{v' v'}(y)$ ,  $\overline{u' u'}(y)$ , and  $\overline{u' v'}(y)$ , in accord with experiments. [Note that  $\dot{\gamma}^2(y)$  displays high-amplitude oscillations [12]; the very low-amplitude oscillations predicted by the model stem from the integrals in (1)–(3), i.e., from the nonlocal character of the model.] The values of  $\xi_v$  and  $\xi_u$  are of

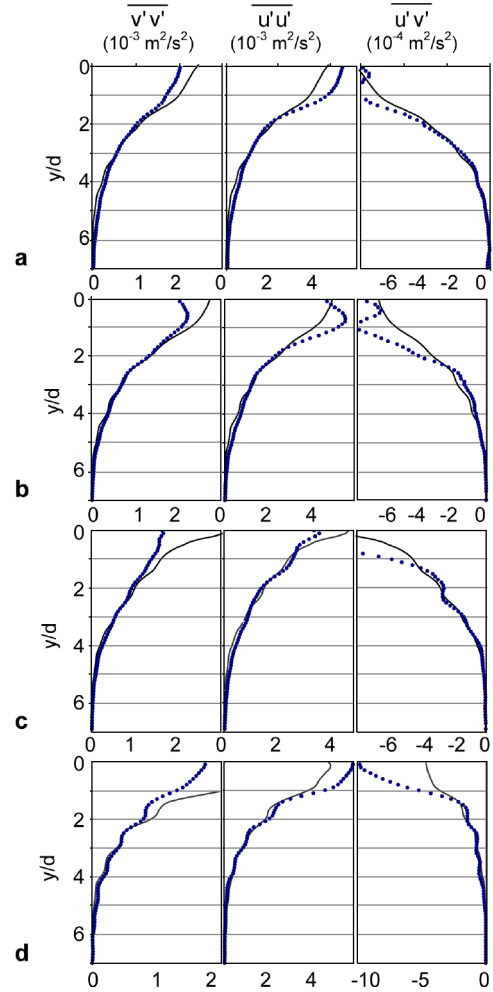


FIG. 4 (color online). Fits of (1)–(3) (solid lines) to the corresponding experimental correlations (points). The fits are limited to the lower part of the flowing layer ( $y > 2d$ ), where the flow is dense and the model applies. (a) Plastic beads,  $d = 2$  mm,  $\omega = 1$  rpm;  $\xi_v = 0.9$ ,  $\xi_u = 1.2$ , and  $\phi = 1.4$  rad. (b) Steel beads,  $d = 2$  mm,  $\omega = 1$  rpm;  $\xi_v = 0.9$ ,  $\xi_u = 1.3$ , and  $\phi = 1.4$  rad. (c) Plastic beads,  $d = 3$  mm,  $\omega = 1$  rpm;  $\xi_v = 0.8$ ,  $\xi_u = 0.9$ , and  $\phi = 1.3$  rad. (d) Plastic beads,  $d = 3$  mm,  $\omega = 1.5$  rpm;  $\xi_v = 0.7$ ,  $\xi_u = 1.0$ , and  $\phi = 1.4$  rad.

order 1, as expected [15]. The small value of  $\cos\phi$  indicates that the correlation is weaker between  $v'$  and  $u'$  than between  $v'$  and itself, in accord with the observation that  $\tau_{\text{Re}} < \sigma_{\text{Re}}$  in the dense flow [Figs. 2(c) and 2(d)].

To test the model further, we obtain  $\xi_v$ ,  $\xi_u$ , and  $\phi$  for a few additional experiments with beads of various types and different angular velocities. We perform the required fits over the lower part of the flowing layer, starting at the same nominal depth as before,  $y = 2d$ , even though there might be variations from experiment to experiment. Yet our results (Fig. 4) indicate that  $\xi_v$ ,  $\xi_u$ , and  $\phi$  are largely independent of the bead type as well as of the angular velocity. We conclude that the fluctuating velocity correlations depend on the variables of a dense granular flow only through  $d$  and  $\dot{\gamma}(y)$ , as evinced by (1)–(3).

To summarize, we have adduced evidence that in dense granular flow the fluctuating velocity may be modeled as the inevitable shaking induced in a stack of wavy strata—an apt description of the structure of the flow—when the strata are made to slip past one another. Based on this model, we have derived Eqs. (1)–(3). The bead diameter appears as a factor on the right-hand sides of (1)–(3), indicating that the fluctuating velocity is a direct manifestation of the granularity of the flow. Although the fluctuating velocity leads to negligible Reynolds stresses in dense granular flow, it can still provide a measure of indirect energy sufficient to drive self-diffusion [16] and segregation—i.e., processes associated with the granularity of the flow [12]. If thought of as a granular temperature, this energy establishes a link between dense granular flow and several problems in which diffusion, creep, magnetization, and other processes are thermally mediated at the atomic or molecular level.

- 
- [1] G.K. Batchelor, *An Introduction to Fluid Dynamics* (Cambridge University Press, Cambridge, England, 1967).  
 [2] H. Tennekes and J.L. Lumley, *A First Course in Turbulence* (MIT Press, Cambridge, MA, 1972).  
 [3] Review articles on granular materials include H.M. Jaeger, S.R. Nagel, and R.P. Behringer, *Rev. Mod. Phys.* **68**, 1259 (1996); T. Shinbrot and F.J. Muzzio, *Phys. Today* **53**, No. 3, 25 (2000).  
 [4] R.A. Bagnold, *Proc. R. Soc. A* **225**, 49 (1954).  
 [5] For simplicity, we assume that the viscosity and the geometry remain invariant. In general, the onset of turbulence is governed by the Reynolds number [2].  
 [6] On the Reynolds stress in granular flows, see P.C. Johnson and R. Jackson, *J. Fluid Mech.* **176**, 67 (1987); P.C. Johnson, P. Nott, and R. Jackson, *ibid.* **210**, 501 (1990).  
 [7] Recent works on the flowing layer in a rotating drum include N. Jain, J.M. Ottino, and R.M. Lueptow, *Phys. Fluids* **14**, 572 (2002); D. Bonamy, F. Daviaud, and L. Laurent, *ibid.* **14**, 1666 (2002).

- [8] Available at <http://glinda.lrsm.upenn.edu/~weeks/idl/download.html>; see also J.C. Crocker and D.G. Grier, *J. Colloid Interface Sci.* **179**, 298 (1996).  
 [9] We partition each of the 1024 images from one experiment into equally sized bins parallel to the  $x$  direction and of thickness  $\delta$  in the  $y$  direction. Consider the bin centered at a depth  $y$ ,  $B_y$  [inset in Fig. 2(a)]. Associated with  $B_y$ , we compute one point of the mean velocity field  $\bar{u}(y) = \bar{u}_{B_y} = (\sum_i \sum_b V_i^b u_i^b) / \sum_i \sum_b V_i^b$ , one point of the mean volume fraction field  $\bar{f}(y) = \bar{f}_{B_y} = \sum_i \sum_b V_i^b / 1024V$ , and one point of, say, the Reynolds shear stress  $\tau_{\text{Re}}(y) = \overline{fu'v'}_{B_y} = \sum_i \sum_b V_i^b (u_i^b - \bar{u}_{B_y}) v_i^b / 1024V$ . Here the sum in  $i$  extends over all 1024 images, the sum in  $b$  extends over all the beads,  $u_i^b$  and  $v_i^b$  are the components of the instantaneous velocity of the bead  $b$  in the image  $i$ ,  $V_i^b$  is the portion of the volume of the bead  $b$  which falls within  $B_y$  in the image  $i$ , and  $V = w\delta d$  (the volume of  $B_y$ ), where  $w$  is the width of the bin in the  $x$  direction. The fields become invariant to changes in  $\delta$  when  $\delta < d/10$ . We use  $\delta = d/20$ .  
 [10] A. V. Orpe and D. V. Khakhar, *Phys. Rev. Lett.* **93**, 068001 (2004).  
 [11] C.R. Calladine, *Plasticity* (Horwood Publishing, Chichester, England, 2000).  
 [12] K.M. Hill, G. Gioia, and V.V. Tota, *Phys. Rev. Lett.* **91**, 064302 (2003); evidence of stratification has also been found in dense granular flow in a Couette apparatus, both experimentally and computationally; see D.M. Mueth, G.F. Debregeas, G.S. Karczmar, P.J. Eng, S.D. Nagel, and H.M. Jaeger, *Nature (London)* **406**, 385 (2000); S.B. Savage and R. Dai, *Mech. Mater.* **16**, 225 (1993).  
 [13] In practice, we compute the integral as a sum over the bins described in Ref. [9].  
 [14] To compute the experimental correlations, we proceed as in Ref. [9]. For example,  $\overline{u'v'}(y) = \overline{u'v'}_{B_y} = (\sum_i \sum_b V_i^b (u_i^b - \bar{u}_{B_y}) v_i^b) / \sum_i \sum_b V_i^b$ . Note that, with this formula and the ones given in Ref. [9],  $\overline{fu'v'}(y) = \bar{f}(y)\overline{u'v'}(y)$ , as it should.  
 [15] The amplitude of the trajectory of stratum  $i$  relative to stratum  $i - 1$  must scale with  $d$ , which implies that  $\xi_v$  and  $\xi_u$  must be of order 1.  
 [16] In dense granular flow, the self-diffusion and the fluctuating velocity are not two aspects of the same phenomenon, as is the case in gaseous flow, where the fluctuating velocity is the velocity of the self-diffusing molecules minus the mean velocity of the flow. In dense granular flow, on the other hand, the fluctuating velocity shakes the particles and impels them to jump between strata (and therefore to self-diffuse) [12]; yet these jumps are infrequent, because they require the presence of voids, which are rare [12], and the velocity associated with the jumps (i.e., with the self-diffusion) can account for only a negligible portion of the fluctuating velocity. In fact, in the absence of voids, the fluctuating velocity would remain virtually unchanged, but self-diffusion would cease. Thus, the self-diffusion and the fluctuating velocity are coupled but distinct phenomena in dense granular flow.  
 [17] T.S. Komatsu, S. Inagaki, N. Nakagawa, and S. Nasuno, *Phys. Rev. Lett.* **86**, 1757 (2001).